



Assessing the fugitive emission of CH₄ via migration along fault zones – Comparing potential shale gas basins to non-shale basins in the UK



I.M. Boothroyd^{a,*}, S. Almond^b, F. Worrall^a, R.J. Davies^b

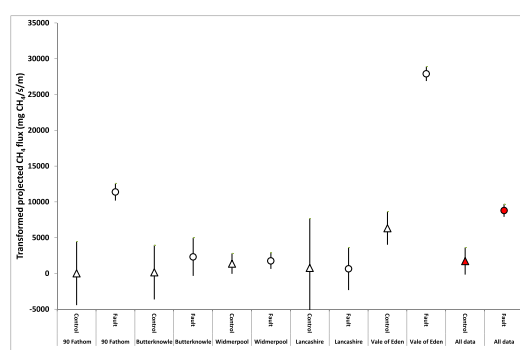
^a Department of Earth Sciences, Durham University, Science Labs, Durham DH1 3LE, UK

^b School of Civil Engineering and Geosciences, Newcastle University, Newcastle NE1 7RU, UK

HIGHLIGHTS

- Fugitive emissions of CH₄ from basin-bounding faults in the UK
- Fault surveys had a significantly higher CH₄ flux than control surveys.
- No apparent link in CH₄ flux to presence or absence of hydrocarbons.
- Estimated flux from faults 11.5 ± 6.3 t CH₄/km/yr

GRAPHICAL ABSTRACT



ARTICLE INFO

Article history:

Received 29 June 2016

Received in revised form 22 August 2016

Accepted 7 September 2016

Available online 1 December 2016

Editor: D. Barcelo

Keywords:

Greenhouse gases

Mobile survey

Hydrocarbons

ABSTRACT

This study considered whether faults bounding hydrocarbon-bearing basins could be conduits for methane release to the atmosphere. Five basin bounding faults in the UK were considered: two which bounded potential shale gas basins; two faults that bounded coal basins; and one that bounded a basin with no known hydrocarbon deposits. In each basin, two mobile methane surveys were conducted, one along the surface expression of the basin bounding fault and one along a line of similar length but not intersecting the fault. All survey data was corrected for wind direction, the ambient CH₄ concentration and the distance to the possible source. The survey design allowed for Analysis of Variance and this showed that there was a significant difference between the fault and control survey lines though a significant flux from the fault was not found in all basins and there was no apparent link to the presence, or absence, of hydrocarbons. As such, shale basins did not have a significantly different CH₄ flux to non-shale hydrocarbon basins and non-hydrocarbon basins. These results could have implications for CH₄ emissions from faults both in the UK and globally. Including all the corrected fault data, we estimate faults have an emissions factor of 11.5 ± 6.3 t CH₄/km/yr, while the most conservative estimate of the flux from faults is 0.7 ± 0.3 t CH₄/km/yr. The use of isotopes meant that at least one site of thermogenic flux from a fault could be identified. However, the total length of faults that penetrate through-basins and go from the surface to hydrocarbon reservoirs at depth in the UK is not known; as such, the emissions factor could not be multiplied by an activity level to estimate a total UK CH₄ flux.

© 2016 The Authors. Published by Elsevier B.V. This is an open access article under the CC BY-NC-ND license (<http://creativecommons.org/licenses/by-nc-nd/4.0/>).

* Corresponding author.

E-mail address: i.m.boothroyd@durham.ac.uk (I.M. Boothroyd).

1. Introduction

With the introduction of high-volume hydraulic fracturing drilling techniques to extract unconventional hydrocarbons from shale formations, there has been increasing concern over the potential contamination of groundwater aquifers and the possible migration of gas and fluids. Some studies have suggested hydraulic fracturing fluids could have migrated to groundwater aquifers along natural fractures (Llewellyn et al., 2015), or that well integrity issues (Davies et al., 2014) have the potential to cause fluid migration to groundwater aquifers from active wells (Ingraffea et al., 2014), possibly as a consequence of poor cementing (Darrah et al., 2014). Fugitive emissions of methane (CH₄) at the ground surface can occur from abandoned wells, whether they have undergone decommissioning (Boothroyd et al., 2016) or remain unplugged (Kang et al., 2014; Townsend-Small et al., 2016). Natural migration of hydrocarbons has been identified along permeable pathways (Grasby et al., 2016; Warner et al., 2012) and Moritz et al. (2015) found deep thermogenic CH₄ could have migrated naturally along faults to aquifers, where it mixed with and was transformed into biogenic CH₄. Lavoie et al. (2016) suggested this process may have also occurred from shallower formations along small scale fracture networks, leading to microbial degradation of thermogenic volatiles in groundwater aquifers. It is important to establish what the cause of groundwater contamination or surface emissions of hydrocarbons is, whether from well integrity issues (Darrah et al., 2014); stimulated fractures connecting to natural faults and fractures (Reagan et al., 2015); or natural migration of fluids (Molofsky et al., 2011). An understanding of baseline conditions is thus required prior to any hydraulic fracturing taking place to determine whether natural seepage occurs.

It is important to understand the extent to which fault zones act as conduits for fluid flow, including hydrocarbons (such as CH₄), and CO₂, when considering the potential impact of hydraulic fracturing processes from shale gas basins. Modelling work has suggested that while fault zones may act as pathways for fluid flow – including frack fluid and brines – (Kissinger et al., 2013; Lange et al., 2013) such a scenario is only likely under certain geological conditions, such as high pressures induced by hydraulic fracturing if a highly permeable ($9.0 \times 10^{-14} \text{ m}^2$) fault zone is present (Kissinger et al., 2013). A study of natural and stimulated hydraulic fractures found the vertical extent of most natural fractures was between 200 and 400 m with a maximum recorded height of 1106 m (Davies et al., 2012). For stimulated fractures in the Barnett, Woodford, Marcellus, Niobrara and Eagle Ford shale gas formations, fracture propagation was typically <100 m and the maximum was 588 m (Davies et al., 2012).

Davies et al. (2013) indicated the maximum height of stimulated hydraulic fractures connecting to pre-existing fractures and hydraulic fractures was 1000 m. It was expected that in the case of stimulated hydraulic fractures in shale basins, overpressure in oil and gas operations would reduce when pumping stops, meaning fractures would be likely to close due to confining stresses. Nonetheless, transmission of fluids through pre-existing fracture systems could not be discounted and consideration of local geology was cited as an important stage prior to allowing fracking operations in a given area (Davies et al., 2013). It is therefore important to consider whether fractures could propagate and connect with larger scale faults, potentially providing pathways for fluid migration if permeability is high, such as with proppant used to keep fractures open under hydraulic fracturing. The importance of vertical separation between stimulated hydraulic fractures and overlying aquifers and the possibility of connections between stimulated and natural fractures allowing fluid flow to overlying aquifers was also highlighted by Jackson et al. (2015), who noted that for ~44,000 wells studied in the USA, the average fracturing depth was 2500 m but 16% were fractured <1600 m and 6% <900 m from the surface. It is consequently important to understand the behaviour of shale basins prior to any hydraulic fracturing processes taking place, so as to understand whether natural leakage of CH₄ and CO₂ from geological

sources already takes place, but also the propensity for fault zones to enhance fugitive emissions following hydraulic fracturing.

To identify whether elevated concentrations of CH₄ in the atmosphere have been transported through fault networks, it is necessary to determine what the source of any elevated concentration is. Indeed, this is a limitation of studies where faults are inferred to transport thermogenic CH₄ but where this is not verified (Voltattorni et al., 2014). Isotopic measurements of $\delta^{13}\text{C}\text{-CH}_4$ can be used to distinguish between thermogenic and microbial sources of CH₄, typically ranging from $\delta^{13}\text{C}\text{-CH}_4\text{-50}$ to -20% and -110 to -50% respectively (Whiticar, 1999). Mobile devices have been effectively used to monitor CO₂ and CH₄ concentrations along with isotopic compositions, enabling the identification of fugitive emissions from urban pipeline leaks (Jackson et al., 2014; Phillips et al., 2013), oil and gas production pads (Brantley et al., 2014) and coal seam gas fields (Maher et al., 2014). Numerous studies have calculated greenhouse gas budgets for shale operations (Burnham et al., 2012; Howarth et al., 2011; O'Donoghue et al., 2014; O'Sullivan and Paltsev, 2012) yet no consideration has been given to the release of thermogenic CH₄ naturally via fault zones and the potential consequence were stimulated hydraulic fractures to connect with natural fractures and provide a permeable pathway for fluid migration to the surface.

There are numerous examples of gaseous migration along fault zones to the surface, both of CH₄ and other gases. In Italy, endogenous migration of CO₂ was found to be greater in grassland with surface expression of faults compared to unfaulted grassland, with an extra soil CO₂ component 0.3–4.0 times background biological soil production of CO₂ (Etiope, 1999). Voltattorni et al. (2014) found peaks in CO₂ and ²²²Rn in Greece were concentrated around fault zones and suggested gas micro-seepage from deep sources through the fault zone was the cause. Similarly, deep-seated faults in Poland have been identified to act as conduits for gas migration – including noble gases, CO₂ and CH₄ (Kotarba et al., 2014). In the Paradox Basin, central Utah, USA, a naturally leaking CO₂ rich system caused enrichment of CO₂ in groundwater, leading to precipitation of travertine mounds from springs and geysers, with vertical migration along faults also transporting hydrocarbons (Dockrill and Shipton, 2010). Migration of CO₂ through fault zones in the Paradox Basin has taken place over hundreds of thousands of years, with enhanced fluid flow concentrating in localised areas rather than across the entire fault system (Burnside et al., 2013). Methane seepage was highly localised along the most permeable sections of faults in Bacau, Romania (Baciu et al., 2008). Geothermal spring temperature measurements have been used as an analogue of convective heat transport along fault zones and evidence of high-permeability flow paths (Fairley and Hinds, 2004). Etiope and Klusman (2002) assessed a range of routes via which CH₄ emissions were possible from fault zones, including: Fischer-Tropsch reactions in geothermal systems; microseepage via buoyant flux of CH₄ or otherwise faults increasing the flow rate of microbubbles; and gas vents. Microseeps have been shown to occur across both onshore and offshore Europe, with estimated fluxes of CH₄ in Europe at 0.8 Tg yr^{-1} and total seepage estimated at 3 Tg yr^{-1} (Etiope, 2009). Faults and fracture networks were suggested to act as preferential pathways of degassing (Etiope, 2009) and Tang et al. (2013) reported hydrocarbon microseepage, including CH₄, through faults in the Yakela condensed gas field in the Tarim Basin, Xinjiang, China. Faults were speculated to act as conduits for coalbed methane migration (Boardman and Rippon, 1997; Creedy, 1988) and have been identified as one of three likely causes of CH₄ migration from coal seams in Ukraine (Alsaab et al., 2009). Furthermore, in the Ruhr Basin, Germany, emissions of thermogenic CH₄ were found where coal bed methane accumulated at the top of Carboniferous sediments (Thielemann et al., 2000). This meant that thermogenic CH₄ emissions were restricted to a few natural faults only, rather than being widespread (Thielemann et al., 2000).

Overpressure can be an important factor affecting fluid migration, with increased pressure driving fluid flow and keeping fractures open

as pressure is higher than minimum principal stress. Birdsell et al. (2015) highlighted topographically driven flow, overpressured shale reservoirs, permeable pathways such as faults or wellbores, increased formation pressure due to hydraulic fracturing fluid injection and the density contrast between hydraulic fracturing fluid to the surrounding brine as possible mechanisms via which hydraulic fracturing fluid could migrate from shale reservoirs to overlying groundwater aquifers. The role of overpressure was discussed by Birdsell et al. (2015) with respect to Osborne and Swarbrick (1997) whereby mechanisms generating overpressure were chiefly: (1) an increase in compressive stress; (2) changes in the volume of the pore fluid or rock matrix; and (3) fluid movement or buoyancy. A model of hydraulic fracturing fluid migration suggested that overpressure could drive a significant amount of fluid flow, dependent upon the effects of well production limiting migration away from the well (Birdsell et al., 2015). Overpressure was also suggested as a mechanism for fluid flow in the South Caspian Basin in a process model for mud volcano systems, whereby overpressure would cause hydraulic fractures to propagate hundreds of metres above the source basin and create pathways for the overpressured fluid to move through the overburden (Stewart and Davies, 2006). Consequently, overpressure could provide a mechanism by which fluid is driven along deep, basin-bounding faults.

In this study, we aimed to test whether deep-seated, through-basin penetrating faults could be conduits for CH₄ migration. Different geological basins are examined, including shale basins, non-shale hydrocarbon basins and a non-hydrocarbon basin, to determine whether there is a difference between fugitive emissions depending upon geology as well. The focus on this study was to examine faults that extend to depth from the surface through hydrocarbon reservoirs rather than leakage through a series of interconnected faults.

2. Methodology

2.1. Study areas

The study was conducted along five fault systems in England (Fig. 1), which are described in detail below. The approach was to consider: two faults bounding potential shale basins; two faults bounding non-shale, hydrocarbon, basins through coal measures; and one fault bounding a basin with no hydrocarbon accumulations, although coal measures were dissected to the west of the basin. The sample size allowed statistical assessment between individual basins but not basin types, this would require multiple fault types within each basin and this is a situation which rarely occurs in nature. Faults were chosen because they were through-basin penetrating; extended from depth to the surface (generally having some identifiable surface expression); and where the basin included hydrocarbon reserves that the fault passes through.

2.1.1. Durham Coal Measures

The 900 m thick Upper Carboniferous Durham Coal Measures are bounded to the north by the Stublick–90-Fathom normal fault system and to the south by the Butterknowle fault system (Fig. 1). The Durham Coal measures extend across the majority of eastern County Durham and form part of the larger Pennine Coal Measures (Fielding, 1984).

The Stublick – 90-Fathom Normal Fault System (herein called 90 Fathom) trends approx. E-W dipping north (De Paola et al., 2005) and forms the northern boundary of the Durham Coal Measures towards the eastern extent of the fault system. The western extent of the system forms the Northern boundary of the North Pennine region and offsets Carboniferous Coal measures of the Northumberland basin (De Paola et al., 2005). The 90 Fathom fault route incorporated Blaydon Quarry landfill, which was accounted for in the data analysis (details below). Cross sections for Stublick and 90 Fathom are available from the British Geological Survey (BGS, 1975; BGS, 1989).

The Butterknowle Normal Fault System (see cross-sections BGS, 1969; BGS, 2008) trends approximately E-W dipping south and

extending from Weardale to the west to the Hartlepool coast in the east (Kortas and Younger, 2013). The fault forms the southern boundary of the Durham coalfield although the coal measures do extend south beyond the fault (Neymeyer et al., 2007). The survey started from the Lunedale fault in Middleton in Teesdale, which is part of the Lunedale-Butterknowle fault system.

2.1.2. Widmerpool Trough

The Widmerpool Gulf is a late-Devonian extensional basin marking the Southern extent of the East Midlands hydrocarbon province. The basin is bounded to the south by the Hoton normal fault system (Church and Gawthorpe, 1994; Fraser et al., 1990). The fault system dips towards the north and trends NW-SE approximately between Ashbourne and Melton Mowbray (Fig. 1). The cross-section of Widmerpool Trough is shown in Fig. 19, Andrews (2013).

The region has a history of oil production with >91 oil wells having been drilled in the surrounding area. The principal hydrocarbon source rocks in the region are the Dinantian and Namurian shales associated with deep water delta systems (Fraser et al., 1990).

2.1.3. West Lancashire

The West Lancashire basin is a sub-basin of the larger oil and gas producing province of the East Irish Sea Basin. The Bowland-Holywell shale units (see cross-section, BGS, 2012) provided the source rocks for the Formby oilfield (Duncan et al., 1998) which began producing in the region in 1939. The Bowland shale is the target for potential shale gas exploration in the region, having been targeted by the Preese Hall well by Cuadrilla in 2011.

The basin is bounded to the east by the west-dipping Lancashire Coalfield Boundary Fault (Jackson and Mulholland, 1993) also referred to as the Western Boundary Fault (BGS, 1977). The fault trends N-S for approximately 32 km (Knott, 1994) between Prescott in the south and Hesketh Bank in the north.

2.1.4. Vale of Eden

The Vale of Eden basin is a half graben formed during Permo-Triassic extension. Regional geology is characterised by Lower Permian Penrith Sandstone, the Upper Permian Eden Shales and the Triassic Sherwood Sandstone Group (Beach et al., 1997). The region has no history of hydrocarbon exploration and is not recognised as having potential for future shale gas operations.

The NW-SE trending basin sits between the Lake District and Alston Blocks and is bounded to the east by the NNW-SSE trending Pennine Fault System (Underhill et al., 1988). The western basin boundary is marked by a system of WNW trending normal faults (Knott, 1994) extending approximately between Penrith and Carlisle and dipping west. There are some coal deposits to the west of the basin (Fig. 1) and a short section of the fault survey was along the west-bounding fault that intersected the coal measures. BGS (1974) provides a cross section of the Vale of Eden basin.

2.2. Gas measurement & analysis

A Picarro Surveyor P0021-S cavity ring down spectrometer (Picarro Inc., Santa Clara, CA) was used to measure CH₄ (precision 5 ppb + 0.05% of reading ¹²C) and δ¹³C-CH₄ (‰, Pee Dee Belemnite) whilst driving along fault and control routes. A sample line was attached to the roof at the back of the vehicle and sample gas was measured at a frequency of 1 Hz. A 2D anemometer (WindSonic, Gill Instruments, Lymington, UK) was attached to the roof of the car (at the front, on a mast ~3 m from ground surface) to measure wind speed (between 0 and 60 m/s ± 2% @ 12 m/s) and direction (0–359° ± 3°), enabling Picarro software to map wind plumes and identify probable source areas. A GPS A21 (Hemisphere, Scottsdale, Arizona) attached to the roof of the vehicle was used to map the location of each measurement. Instrument and GPS alignment was undertaken during

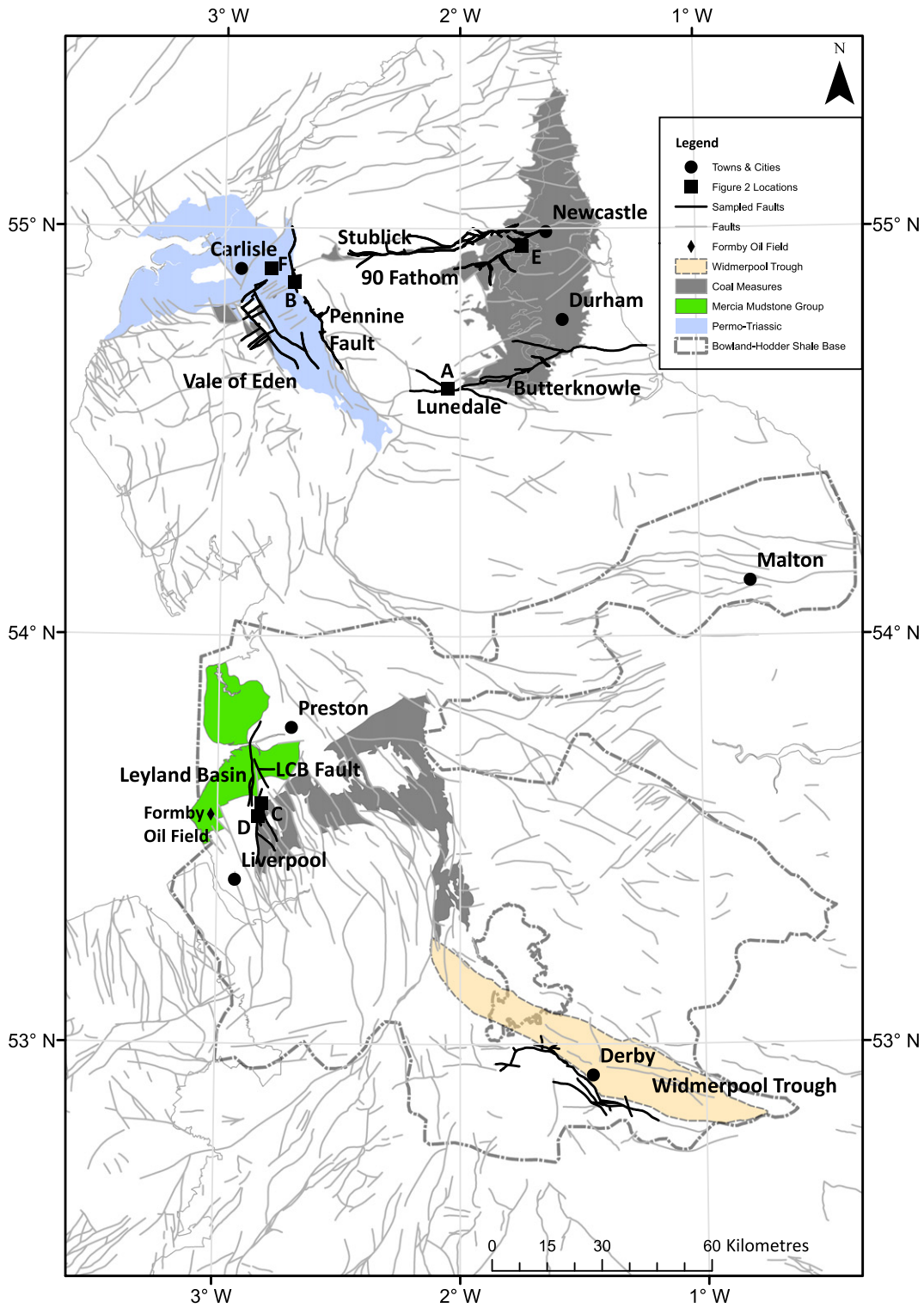


Fig. 1. Map of study faults and regional geology. LCB Fault is the Lancashire Coalfield Boundary Fault. Permo-Triassic refers to the Vale of Eden basin. Labels A–F refer to panels in Fig. 2. Widmerpool Trough based upon Andrews (2013), with the permission of the British Geological Survey. Faults and bedrock reproduced with the permission of the British Geological Survey ©NERC. All rights Reserved.

installation to correct for delays between sample detection and GPS logging due to sample tube length.

Methane concentration, land use and fault data were mapped in ArcMap. The raw concentration data was downloaded from the surveyor and converted into ArcMap (version 10) point shapefiles. Using the point shapefiles of raw CH₄ concentration, individual fault and control survey route lengths were calculated at Ordnance Survey (OS)

1:25,000 scale. A total of 783.5 km were travelled along the five fault and control routes. Fault and control route lengths were used to determine the number of peaks measured by the surveyor per km travelled. The Picarro Surveyor automatically identified elevated CH₄ concentrations, which were determined relative to ambient background – here referred to as peaks. A minimum amplitude of 0.1 ppmv was used to identify peaks above ambient background in a given locality;

0.1 ppmv was the standard setting and conservative, as 0.03 ppmv is the lowest recommended setting for natural gas leaks. Land use at the location of each elevated concentration was determined using the 2007 OS 25 m land use classification – typically they were grassland, urban or suburban. The classification did not provide information on faults or hydrocarbon basins. Faults were mapped using British Geological Survey 1:50,000 geology data in ArcMap, which was the best resolution dataset available for all study areas. From this, surveyed faults and faults connected to them in the ArcMap shapefile that were traversed were mapped and the distance between a given elevated concentration and the fault calculated to the nearest metre. Suitable faults were selected based on literature, geological maps and cross-sections showing faults, basins and hydrocarbon deposits that fitted the criteria outlined in the aims. For control routes, the median line was mapped and the distance between it and CH₄ concentrations measured. Concentration data points included the GPS location that was recorded, not the location of the source of the methane (e.g. the fault or a farm).

Fault and control routes were revisited within two days of the initial survey for detailed isotopic measurements. Areas identified as having elevated CH₄ concentrations were selectively revisited based on time constraints and allowing similar numbers of measurements between fault and control routes. Areas revisited were usually based on elevated concentration locations identified as peaks above local ambient by the Picarro Surveyor software, but limited mobile wi-fi signal strength meant data could not always be processed by the surveyor and uploaded to an online cloud store to be assessed by the end user, meaning elevated concentrations identified in the raw data files were used instead. Due to practical limitations, it was not always possible to park at the exact location an elevated concentration was determined (for instance it was not possible to stop and park on high-speed roads), so sites were selected based on suitability and safety when stopping for prolonged periods. Isotopes were measured for a period of 10 min from real-time atmospheric sampling while the vehicle remained stationary at a given location. The isotope composition was determined using Keeling plots of $\delta^{13}\text{C}-\text{CH}_4$ against the inverse of CH₄ concentration, with the intercept representing the source composition (Pataki et al., 2003).

2.3. Data analysis

Data were censored relative to the wind direction. Because the position of the fault, or the selected control line, was known relative to the wind direction it was possible to remove any concentration or isotopic data for which the sensors were not downwind of the potential source. For fault routes, isotopic data is presented for complete 10 min analytical periods described above and wind resolved data, with data when the wind direction was not from the fault, removed. Data were examined for peaks above ambient concentration lying on or close to the fault, with the wind direction from across the fault and with an isotopic signal consistent with a thermogenic source. The data were tested using two statistical approaches. Binary logistic regression was used to assess specifically the likelihood of an elevated CH₄ concentration occurring on a fault route or from a particular basin. Analysis of variance (ANOVA) was used to assess significant differences between concentrations and fluxes from faults and controls and basins. Mobile surveys provide thousands of datapoints and this paper adopts two approaches to data analysis to provide a methodological assessment for such datasets. Any data collected whilst the wind was in the opposite half-disk (outside of 90° either side of the datapoint) from the nearest point on the fault or control was removed prior to ANOVA and CH₄ flux determination, but not prior to binary logistic regression (details below). Similarly, prior to any analysis, prolonged stationary periods (primarily when changing batteries to the Picarro Surveyor) were removed from analysis as it was a mobile survey and they were not surveying different sections of the fault or control, but periods in stationary traffic were not excluded.

2.3.1. Binary logistic regression

Binary logistic regression was used to separate methane concentrations into background (0) and elevated (1) concentrations and assess the probability of elevated CH₄ concentrations occurring along faults or in basins. The 90th percentile of CH₄ concentration data was used to separate background and elevated concentrations as it has been used to derive urban pipeline leaks (Phillips et al., 2013). Furthermore, when tested with the 95th percentile, some faults were excluded from the analysis as CH₄ concentrations did not exceed the 95th percentile, thus the 90th percentile was used. All concentrations >90th percentile were given a score of 1. The 90th percentile was derived from wind-corrected fault data and complete control data. Complete control datasets were included in binary logistic regression so as not to exclude basins from the analysis when wind-corrected control routes did not have scores above the threshold for separating background and elevated concentrations.

Binary logistic regression was analysed in Minitab (version 17) using the logit link function:

$$g(p_i) = \log\left(\frac{p_i}{1-p_i}\right) \quad (1)$$

where: g = the logit function and p_i is the observed probability of level i of the categorical response variable (Hosmer and Lemeshow, 2000). The response variable was the binary scores of 0 and 1 given to CH₄ concentration data. Two factors were tested in the model as categorical predictors to explain variation in the response variable: Basin (five factor levels: Butterknowle, 90 Fathom, Vale of Eden, Lancashire, Widmerpool); and Target (two factor levels, fault or control). Basin type (shale, coal measures, non-hydrocarbon) could not be estimated by the model and was removed from the analysis. Thus, Basin and Target were used to explain variation between background and elevated CH₄ concentrations. Odds ratios between Basin factor levels and Target factor levels were compared to determine the likelihood of a given Basin or Target having elevated CH₄ concentrations when compared to another. Two separate analyses were conducted; one including a section along the 90 Fathom fault route within the vicinity of a landfill; and with the landfill section removed entirely. This was done for two reasons: (1) the landfill was included as it had high concentrations of CH₄ and it was important to determine its impact; and (2) the purpose of the study was to assess the influence of faults so the landfill was excluded to more effectively establish the difference (if any) between fault and control targets. The 90th percentile was derived from the landfill excluded dataset, so that high concentrations associated with the landfill did not bias determination of elevated concentrations along faults. Models were checked for co-linearity using variance inflation factors (VIFs), where VIFs > 5 were considered to indicate co-linearity and in such circumstances a different reference fault was chosen to reduce co-linearity.

2.3.2. Correcting concentration with distance

During the surveys it was not possible to stay a fixed distance from the fault (or control line) and with distance any concentration of methane would expect to decline to ambient, therefore, any difference between basins, or between faults and controls could be ascribed to the distance away from the survey line at each point of measurement. Therefore, the data needed to be controlled for the distance away from the survey line. To do this the dynamic plume approach of Hensen and Scharff (2001) was used. A 3D Gaussian plume model was applied to the data from the days of each fault or control survey. Data were first corrected for the ambient concentration measured on that day and concentration data, recorded as ppmv were converted to mg/m³ with knowledge of the air pressure and temperature conditions on the day. A 3D Gaussian plume was then used to predict the flux above the projected fault or control survey line (Q – Eq. (2)) given the concentration of methane above ambient at a point a known distance

away – the 3D plume model is:

$$\text{Conc.}(x, y, z) = \frac{Q}{2\pi u_x \sigma_y \sigma_z} e^{-\frac{y^2}{(2\sigma_y)^2}} \left[e^{-\frac{(z-H)^2}{(2\sigma_z)^2}} + e^{-\frac{(z+H)^2}{(2\sigma_z)^2}} \right] \quad (2)$$

where: x = shortest distance from point of measurement to the fault (m); y = the perpendicular distance along the fault of the measurement (zero m in this study); z = the height of the detector above the ground surface (1.5 m); Q = the source strength (mg/s); u = the wind speed resolved along x (m/s); H = the height of the source (m); and σ_y and σ_z = dispersion terms in the directions y and z . The dispersion terms are approximated as $\sigma_y = I_y x$, and $\sigma_z = I_z x$ and in near surface conditions we assume that there is no stable stratification and that therefore $I_z = I_y = 0.5$. The shortest distance to the fault from the point of measurement was calculated (x) and given the measurement of the wind speed and direction at height z then the wind speed could be resolved along direction of the shortest distance to the fault (u_x). Note that data collected when the wind was in the wrong half-disk were already removed prior to analysis for fault distance. The methane release at the source was assumed to be passive and diffusive, there is no reason to believe that the gas from a fault would be released under pressure and so not released at speed, and so $H = 0$ and no allowance for buoyant lift-off was allowed for. By this approach the measured methane concentration above ambient (C) is adjusted to a supposed source at some distance x and angle away from the measurement. This approach means that any source of methane is assumed to be from a fault and so it was important that the data from the control line was treated in the same way. For the survey on the control the data was corrected using Eq. (1) when instead of a fault a line that was taken as the assumed source the median line of the control survey was used. If the fault is a source of methane then it would be expected that the concentrations corrected to the fault would be significantly greater than those for the control survey corrected to a median line.

The data were also corrected for the distance travelled along the fault or median control line. While the surveys were being conducted it was often the case that the car was stationary for periods of time and so multiple measurements were made at one location - thus weighting for the distance travelled between recorded data removes those multiple measurements at the same location.

2.3.3. Analysis of variance

The survey design used in this study was established as a factorial design and so it was appropriate to use analysis of variance (ANOVA). The ANOVA was considered with two factors. The first factor was the basin with five levels (90 fathom, Butterknowle, Vale of Eden, Lancashire and Widmerpool), and the second factor was the nature of the source (target) which had two levels – fault or control. Given the design it was possible to consider the interaction between these two factors, and therefore use this term to assess whether there was a significant difference between each fault survey and its respective control survey.

Prior to ANOVA the wind direction corrected data were censored for data that was below or at ambient CH₄ concentration. Further the data were Box-Cox transformed to assess for outliers and removed if present. The data were then tested for normality using the Anderson-Darling test (Anderson and Darling, 1952) and it proved necessary to transform the data as its squared reciprocal. The Levene test was used to test for the homogeneity of variance. The Tukey test was used post hoc to assess where significant differences lay between factor levels. The proportion of variance explained by factors was assessed by the generalized ω^2 (Olejnik and Algina, 2003). To avoid type I errors all probability values were assessed as significant if the probability of difference from zero is >95%, but if the probability is close to this value then it is reported. Results were expressed as least squares means as these are better estimates of the mean for that factor level having taken account of the other factors and interactions that were included in the analysis. The

ANOVA was applied to three sets of the data: the ambient concentration data; the projected flux; and the distance weighted projected flux.

Once significant sources had been identified using this process the data were used to measure the flux from the faults.

3. Results

Most of the mean concentrations of CH₄ (Table 1) were at atmospheric background concentrations of ~1.8–1.9 ppmv CH₄. Exceptions to this were on the 90 Fathom Fault route (2.24 ppmv CH₄) and the Vale of Eden fault (2.20 ppmv CH₄) and control (2.26 ppmv CH₄) routes. Mean CH₄ concentration for the 90 Fathom fault route was at atmospheric background levels when the landfill data was excluded. The maximum concentration detected was 13.73 ppmv CH₄ around the landfill, with the next highest concentration on the Vale of Eden control, 6.86 ppmv CH₄. When only wind corrected data greater than the 90th percentile is included, the sample size is reduced. The 90 Fathom fault route including landfill data had 692 data points > 2.21 ppmv CH₄, while the Vale of Eden had 2234 and 1998 on the fault and control routes respectively. The next highest sample size was 14 data points on the Butterknowle control.

3.1. Elevated concentrations and isotopic composition

Over 783.5 km driven, a total of 139 elevated concentrations were detected across the five basins surveyed, with 70 and 69 for fault and control routes respectively (Table 2). For two routes, the 90 Fathom fault route and Vale of Eden control, the number of detections were particularly large, with 21 and 37 respectively. Thirteen of the elevated concentrations detected on the 90 Fathom fault route were in the vicinity of Blaydon Quarry landfill, including two with concentrations above 10 ppmv (Fig. 2E). For the Vale of Eden control, 23 peak concentrations were detected whilst driving up and down ~2.6 km of road. Methane concentrations along this part of the control ranged from 2.53–6.52 ppmv, with a mean of 3.43 ppmv. For two basins, 90 Fathom and Widmerpool, more peaks were detected on the fault route than the control, while the reverse was true for the Vale of Eden. The fault and control routes of Butterknowle and Lancashire had the same number of peak concentrations. Controls had a greater number of peaks per km travelled for three of the five routes, with 0.72 peaks km⁻¹ on the Vale of Eden the maximum rate.

3.1.1. Fault peaks

The Butterknowle fault route included an elevated concentration (2.32 ppmv CH₄, Fig. 2A – note Fig. 2 shows raw wind-corrected concentrations rather than Picarro Surveyor peak concentrations) 19 m from the fault and the source direction was towards the fault. The land use was acid/improved grassland adjacent to houses and farmland. It was not possible to get a $\delta^{13}\text{C}$ -CH₄ measurement to confirm the isotopic source of the CH₄. The second closest peak (3.77 ppmv CH₄) to the fault was 69 m away, but was located on a major road where it was not possible to stop and so no isotopic measurement was taken. A 2.05 ppmv peak located 178 m from the fault had an isotopic signature of -37% $\delta^{13}\text{C}$ -CH₄ indicating a thermogenic source (High Etherley, Fig. S.I.1). When wind resolved, the source composition was -39% $\delta^{13}\text{C}$ -CH₄ (Fig. S.I.2) but the location was in a suburban area, so may have been from a local gas leak.

A peak (2.08 ppmv) 11 m from the 90 Fathom fault was repeated on the isotope sampling day, with a 3.71 ppmv peak 2 m from the fault near Corbridge. It was not possible to perform an isotopic measurement at this site, but a thermogenic signature was observed 44 m from the fault near Corbridge railway station (Fig. 3), though the wind direction was not towards the fault. This site did not have an elevated concentration identified by the software on the first sample day, but did have concentrations above background levels on the isotope sampling day, including two <10 m from the fault.

Table 1
Descriptive statistics for fault and control of each basin. SE = standard error.

Data type	Target	Route	N	Mean	SE Mean	Minimum	Maximum	
Complete fault and control routes	Widmerpool	Control	5399	1.91	0.000503	1.89	3.24	
		Fault	8313	1.91	0.000395	1.89	2.80	
	Lancashire	Control	4153	1.88	0.0013	1.85	4.93	
		Fault	5568	1.88	0.00041	1.87	3.18	
	Butterknowle	Control	5547	1.87	0.000433	1.86	2.63	
		Fault	9283	1.87	0.000342	1.86	3.97	
	90 Fathom	Control	5442	1.88	0.000386	1.86	2.70	
		Fault landfill	9374	2.24	0.0151	1.86	13.73	
		Fault no landfill	8537	1.89	0.000452	1.86	2.52	
	Vale of Eden	Control	4167	2.26	0.00461	1.89	6.86	
		Fault	8428	2.20	0.00169	1.87	4.88	
	Datapoints >90th percentile	Widmerpool	Control	11	2.52	0.114	2.22	3.24
			Fault	5	2.34	0.0579	2.24	2.56
		Lancashire	Control	8	3.51	0.34	2.23	4.93
Fault			6	2.56	0.139	2.32	3.18	
Butterknowle		Control	14	2.34	0.0329	2.22	2.63	
		Fault	3	2.34	0.0233	2.29	2.36	
90 Fathom		Control	8	2.45	0.0658	2.26	2.70	
		Fault landfill	692	5.74	0.119	2.21	13.73	
		Fault no landfill	11	2.25	0.0101	2.21	2.31	
Vale of Eden		Control	1998	2.44	0.00757	2.21	6.86	
		Fault	2234	2.32	0.00188	2.22	3.23	

In the Vale of Eden, the non-hydrocarbon basin, the closest peak (2.10 ppmv, Fig. 2B) detected to the fault was 31 m away, with the source area including the fault. The location was on farmland of improved grassland but neither a thermogenic nor biogenic source could be confirmed. Two elevated concentrations from the Lancashire fault route (2.37 and 3.01 ppmv CH₄, Fig. 2C, D) were located 87 m from the fault. Both were included in the wind corrected dataset, but isotopic composition could not be determined for either location relative to their source area. In the Widmerpool shale basin, five elevated concentrations were within 100 m of the fault. The closest was not towards the fault and no isotopic signature could be identified. For two more elevated concentrations, the source direction was towards the fault but the field of view incorporated agricultural fields (including Pear Tree Farm, Fig. S.I.1, Fig. S.I.2). Another elevated concentration was located 75 m from the fault and the source area was towards the fault. This was a residential area and a distinct isotopic composition could not be determined.

3.1.2. Non-fault peaks

More than half the peaks on the 90 Fathom fault route were within the vicinity of Blydon Quarry landfill (2.58–11.61 ppmv CH₄, Fig. 2E), with an isotopic signature of -61% $\delta^{13}\text{C}-\text{CH}_4$ (Fig. 3). Biogenic sources were predominantly from farmland, including Widmerpool Pear Tree Farm (-74% $\delta^{13}\text{C}-\text{CH}_4$), Lancashire Skelmersdale (-74% $\delta^{13}\text{C}-\text{CH}_4$) and Vale of Eden Birchwood Farm (-57% $\delta^{13}\text{C}-\text{CH}_4$), which had a 3.22 ppmv CH₄ concentration (Fig. S.I.1, Fig. S.I.2). Five thermogenic sources were identified, two on fault routes (one of which was in a suburban area) and three from control routes, suggesting that localised gas

leaks from the public supply were more easily identified than any gas migration to the surface from major faults. This included 23 elevated concentration peaks (2.53–6.52 ppmv CH₄) on the Vale of Eden control at Corby Hill (Fig. 2F).

To summarise, one distinct instance has shown a thermogenic CH₄ signature close to a major fault. Elevated concentrations of CH₄ were also detected close to faults at other locations, but the isotopic composition of the gas could not be confirmed. Elevated concentrations from farmland and landfill constituted distinct biogenic sources of CH₄ and had greater CH₄ concentrations than fugitive emission from faults.

3.2. Binary logistic regression

The 90th percentile was 2.21 ppmv CH₄ and with the landfill-inclusive dataset there were 39,231 datapoints \leq 2.21 (binary score 0) and 4979 datapoints $>$ 2.21 (binary score 1). The best-fit model passed Deviance ($p = 1.000$) but failed the Pearson ($p < 0.0005$) and Hosmer-Lemeshow ($p < 0.0005$) goodness of fit tests. Basin and Target were both significant ($p < 0.0005$) in the binary logistic regression (deviance R^2 adjusted 43.26%). For Target, the odds ratio was 1.72, indicating that fault routes were 72% more likely than control routes to have elevated CH₄ concentrations.

Vale of Eden was used as the reference basin and the negative coefficients (Table 3) indicated that all other basins had a lower likelihood than the non-hydrocarbon control basin of having elevated CH₄ concentrations. This difference was reflected in the odds ratios (Table 4), with the lowest (Butterknowle) and highest (90 Fathom) having just 0.017% and 8.1% of the odds of Vale of Eden for elevated CH₄ concentrations

Table 2
Elevated concentrations detected for fault and control routes by basin and number of crossings of fault or control median line.

Basin	Target	Distance (km)	Number of peaks	Peaks/km	Number of crossings	Crossings/km
Widmerpool	Control	72.189	4	0.06	34	0.47
	Fault	81.569	15	0.18	67	0.82
Lancashire	Control	45.16	8	0.18	26	0.58
	Fault	53.711	8	0.15	33	0.61
Butterknowle	Control	79.55	12	0.15	38	0.48
	Fault	112.976	12	0.11	54	0.48
90 Fathom	Control	81.794	8	0.10	42	0.51
	Fault	109.044	21	0.19	69	0.63
Vale of Eden	Control	51.225	37	0.72	29	0.57
	Fault	96.314	14	0.15	69	0.72

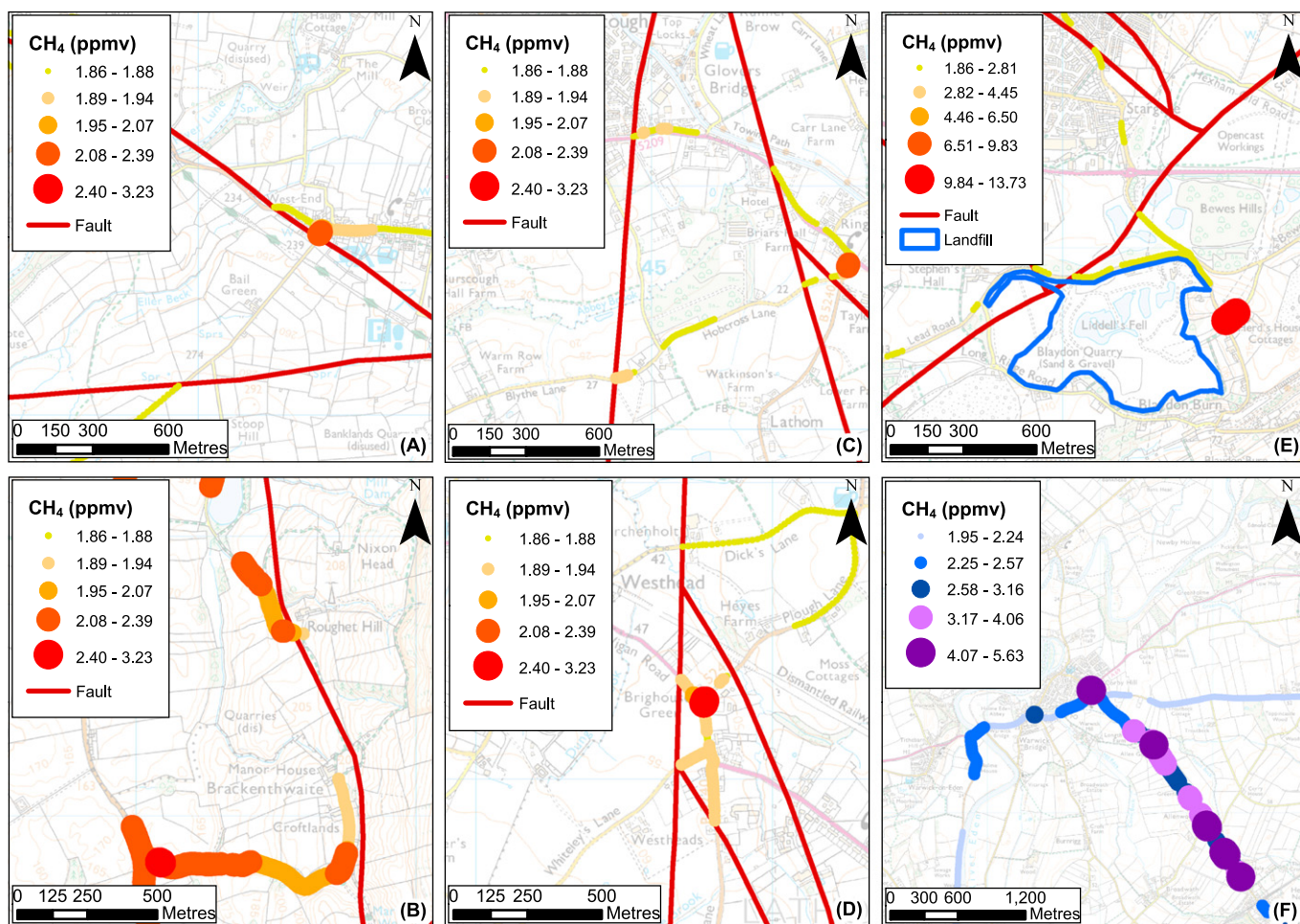


Fig. 2. Wind corrected methane concentrations for fault (yellow-red) and control (blue-purple) routes: (a) Butterknowle fault; (b) Vale of Eden fault; (c) & (d) Lancashire fault - shale basin; (e) 90 Fathom fault; and (f) Vale of Eden control. Panels E–F have separate scales due to the large range in concentrations. © Crown Copyright and Database Right [2016]. Ordnance Survey (Digimap Licence). Faults reproduced with the permission of the British Geological Survey ©NERC. All rights Reserved

respectively. The 90 Fathom had the second highest likelihood of elevated concentrations of CH₄, with odds ratios 28, 42 and 47 times higher than the Lancashire shale, Widmerpool shale and Butterknowle coal basins respectively. The odds ratios for the Lancashire and Widmerpool shale basins indicated significantly higher odds of elevated CH₄ concentrations than Butterknowle, but the confidence intervals ranged from less than to > 1, suggesting this pattern was not certain.

Excluding landfill data from the analysis, 39,217 datapoints had a binary score ≤ 2.21 and 4298 datapoints had a score > 1. The final model included Basin ($p < 0.005$) as the only predictor and passed all goodness of fit tests (Deviance $p = 1.000$, Pearson $p = 0.492$, Hosmer-Lemeshow

$p = 1.000$). Deviance R^2 adjusted was 53.42%. The insignificance of Target indicated that elevated concentrations of CH₄ on the fault route (Table 4) were attributable to emissions from the landfill and not from upward migration of CH₄ along faults. Without the landfill data, there was no significant difference between fault and control routes. The odds ratios for the 90 Fathom coal basin having elevated concentrations of CH₄ changed (Table 5) and the 95% confidence intervals indicated no clear pattern between the 90 Fathom and other hydrocarbon basins. Given the significantly greater odds of the non-hydrocarbon control basin having elevated concentrations of CH₄ compared with coal and shale basins, results indicate that the influence of both major

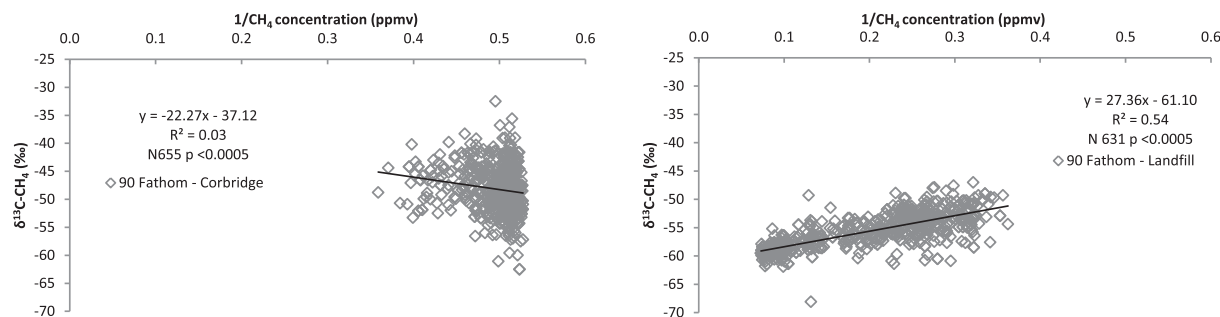


Fig. 3. Keeling plots of $\delta^{13}\text{C-CH}_4$ from 90 Fathom. Source composition is from y-intercept. N = sample size. p value refers to regression. Fault route shown as diamonds. Note the high CH₄ concentrations indicate a microbial source for the landfill site.

Table 3

Binary logistic regression coefficients (Coef). SE = standard error; VIF = variance inflation factor. Basins relative to Vale of Eden, Target relative to control.

Model	Term	Coef	SE coef	VIF	
Including landfill	Constant	-0.349	0.0294		
	Basin				
	Lancashire	-5.864	0.269	1.00	
	Widmerpool	-6.256	0.251	1.00	
	Butterknowle	-6.371	0.244	1.00	
	90 Fathom	-2.5168	0.0449	1.01	
	Target				
	Fault	0.5438	0.0377	1.00	
	Excluding landfill	Constant	-0.0632	0.0214	
		Basin			
Lancashire		-5.962	0.268	1.00	
Widmerpool		-6.283	0.251	1.00	
Butterknowle		-6.363	0.244	1.00	
90 Fathom		-6.128	0.231	1.00	

faults and hydrocarbons is limited compared to other factors such as land use (e.g. farming) and fugitive emissions, such as the natural-gas pipeline emissions suspected as detected on the Vale of Eden control.

3.3. Analysis of variance

The amount of data available to the ANOVA and the distance of survey line involved are detailed in Table 6. When only corrected for the data where the wind was not in the same half-disk as the fault (wind corrected – Table 6) then 40,152 could be considered, this number of datapoints decreased by almost half when the data were corrected for the ambient CH₄ conditions (Table 6 – Ambient corrected) and to 14,180 data points when corrected for the distance travelled along the survey line (Distance corrected), i.e. 7390 datapoints were recorded when the vehicle had not moved any further distance along the survey line from the previous datapoint. The projection of the data to the survey line does not result in any removal of datapoints.

When considered relative to the measured concentrations above the ambient on the day (Table 6 – Ambient corrected), the ANOVA shows that there were significant differences between all basins; between the target (control and fault lines); and the interaction between the two of them. The most important factor was basin (explaining 33% of the original variance). Post hoc analysis shows that there were significant differences between all basins with the Vale of Eden showing the largest values above ambient and Lancashire showing the lowest. This factor is most likely to reflect differences between days of sampling, for example a variable wind speed causing a greater number of gusts and so more data above ambient. The difference between survey line type (target factor) was significant but only explained 5% of the original variance, but given the sampling size even such a small effect was discernible. The least squares mean of the control line had a lower

Table 4

Binary logistic regression odds ratios including landfill data. Odds refer to likelihood of level A having more elevated CH₄ concentrations than level B. CI = confidence interval.

Level A	Level B	Odds ratio	95% CI
Basin			
Lancashire	Vale of Eden	0.0028	(0.0017, 0.0048)
Widmerpool	Vale of Eden	0.0019	(0.0012, 0.0031)
Butterknowle	Vale of Eden	0.0017	(0.0011, 0.0028)
90 Fathom	Vale of Eden	0.0807	(0.0739, 0.0881)
Widmerpool	Lancashire	0.6753	(0.3293, 1.3848)
Butterknowle	Lancashire	0.6018	(0.2964, 1.2220)
90 Fathom	Lancashire	28.4106	(16.7182, 48.2804)
Butterknowle	Widmerpool	0.8912	(0.4500, 1.7649)
90 Fathom	Widmerpool	42.0712	(25.6079, 69.1189)
90 Fathom	Butterknowle	47.2098	(29.1552, 76.4450)
Target			
Fault	Control	1.7225	(1.5999, 1.8546)

Table 5

Binary logistic regression odds ratios excluding landfill data. Odds refer to likelihood of level A having more elevated CH₄ concentrations than level B. CI = confidence interval.

Level A	Level B	Odds ratio	95% CI
Basin			
Lancashire	Vale of Eden	0.0026	(0.0015, 0.0044)
Widmerpool	Vale of Eden	0.0019	(0.0011, 0.0031)
Butterknowle	Vale of Eden	0.0017	(0.0011, 0.0028)
90 Fathom	Vale of Eden	0.0022	(0.0014, 0.0034)
Widmerpool	Lancashire	0.7257	(0.3539, 1.4879)
Butterknowle	Lancashire	0.6696	(0.3298, 1.3594)
90 Fathom	Lancashire	0.8471	(0.4244, 1.6907)
Butterknowle	Widmerpool	0.9227	(0.4660, 1.8273)
90 Fathom	Widmerpool	1.1673	(0.5999, 2.2713)
90 Fathom	Butterknowle	1.265	(0.6571, 2.4352)

concentration than that for the fault line. The interaction term explained 11.9% of the original variance and the post hoc analysis showed that there was a significant difference between the fault and control lines for all the basins except for the Widmerpool basin; in all the cases where there was a significant difference the fault gave a higher concentration than the control.

When the data was projected to the fault or median control line, i.e. the data is distance corrected, then all factors and the interaction were still significant. The difference between basins was still the most important factor (explaining 19% of the original variance), but now there was no significant difference between the 90 Fathom and Widmerpool basins and between the Butterknowle and Lancashire basins. There was still a significant difference between fault and control surveys with fault surveys being significantly higher sources. When the interaction term was examined then there were significant differences between the fault and control surveys in the 90 Fathom, Butterknowle, Widmerpool and Vale of Eden basins but no difference for the Lancashire basin. For the 90 Fathom, Butterknowle and Vale of Eden basins the fault line was significantly larger than the control line, but for the Widmerpool basin the control line was larger than the fault line.

When projected to the fault or control line and distance weighted along the route travelled then there was a significant difference between basins (Fig. 4). The 90 Fathom and Vale of Eden basins were significantly different from each other and significantly higher than the other basins (Butterknowle, Lancashire and Widmerpool) which were, in turn, not significantly different from each other. There was a significant difference between the fault and control survey lines with faults being significantly higher (Fig. 4). When the interaction between factors was considered then there were only significant differences between the fault and the control for only the Butterknowle, 90 Fathom and Vale of Eden, and in no case for any basin was the distance weighted result higher for the control than for the fault, i.e. the reason that the control line for the Widmerpool basin appeared to have significantly higher

Table 6

Sample size (n) and distance travelled (km) for wind corrected, ambient corrected and distance corrected datasets. For explanation of terms (Wind corrected; Ambient corrected and Distance corrected) refer to the text.

Basin		Wind corrected		Ambient corrected		Distance corrected	
		n	Distance	n	Distance	n	Distance
90 Fathom	Fault	4554	50	2156	11	1450	11
	Control	2612	77	843	18	761	18
Butterknowle	Fault	7639	62	417	3	260	3
	Control	4252	4	1150	11	732	11
Vale of Eden	Fault	8428	75	8204	59	4033	59
	Control	1984	25	806	10	778	10
Widmerpool	Fault	3742	77	3742	35	3379	35
	Control	3857	112	3857	34	2459	34
Lancashire	Fault	1693	16	260	2	189	2
	Control	1691	19	139	1	139	1
Total		40,152	346	21,574	254	14,180	254

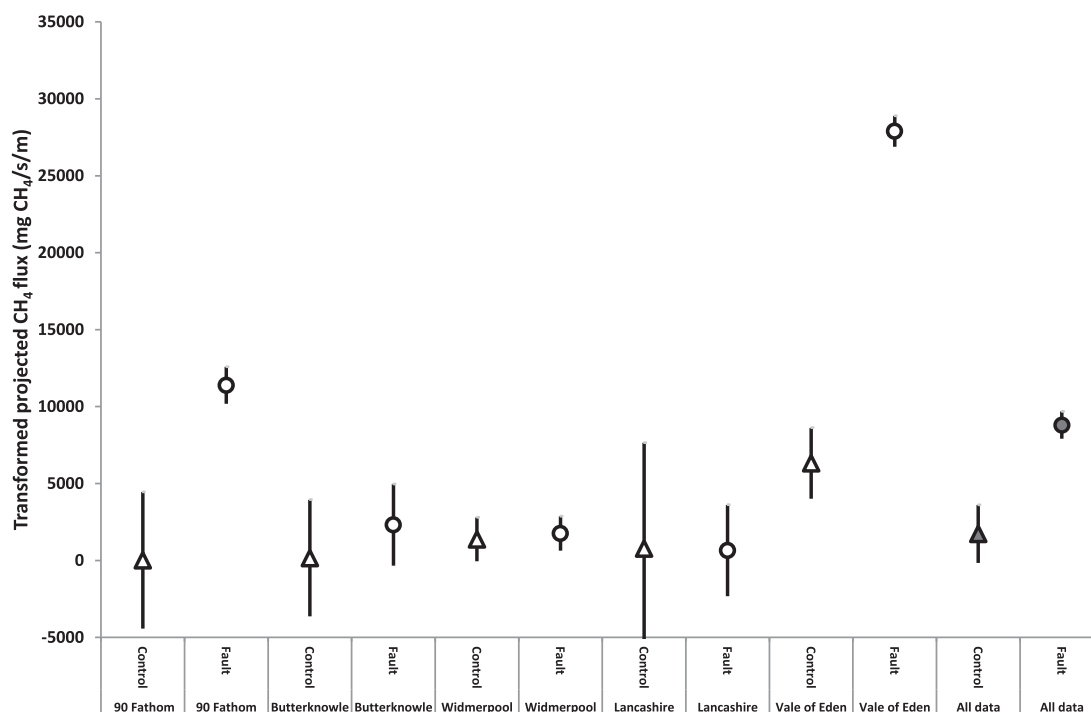


Fig. 4. The main effects plot of the transformed, projected (i.e. distance-weighted) CH₄ concentrations least squares means and their standard errors for the interaction between the basin and type alongside the main effects for the type factor (labelled 'All data').

CH₄ fluxes in previous ANOVA was that any high CH₄ fluxes were over relatively short distances along the survey lines.

3.4. Flux from faults

Given the results for the faults when corrected for wind-direction, distance from the fault; distance along the fault; and corrected for the ambient CH₄ concentration on the sampling day deep basin bounding faults are a source of 0.37 ± 0.20 mg CH₄/m/s of fault (11.5 ± 6.3 t CH₄/km/day). However, this flux is concentrated onto certain locations on certain faults and this result is entirely dominated by results from the Vale of Eden. When the flux values for the Vale of Eden are removed and it is assumed that faults or control lines cannot be a net sink of CH₄ (few locations on Earth are CH₄ sinks) then the result is 0.49 ± 0.66 mg CH₄/m/s (0.7 ± 0.3 t CH₄/km/day). This better represents the observation that for some faults or basins there was not a significant difference between control lines and the fault bounding the basin. Furthermore, if we consider that a fault cannot be a sink of methane then the result becomes 0.00 to 0.03 mg CH₄/m/s with a median of 0.02 mg CH₄/m/s, this would scale to 0 to 1.1 t CH₄/km/yr with a median of 0.7 t CH₄/km/yr. For individual faults the flux due to fault was taken as the difference between the least mean squares for the fault and control

Table 7

The estimated flux from each fault where: A. based upon all basin, projected and distance weighted data; and B. projected, distance weighted data having removed data from the Vale of Eden and assuming no fault could be a sink of CH₄. The error is given as the 95% confidence interval. Fluxes are in terms of fault length of km driven and distances are not corrected for topography.

Basin	Fault flux (t CH ₄ /km/year)	
	A.	B.
90 Fathom	2.9 ± 1.2	2.8 ± 1.2
Butterknowle	1.3 ± 0.7	1.2 ± 0.7
Vale of Eden	52.1 ± 36.7	na
Widmerpool	2.0 ± 1.9	2.0 ± 1.8
Lancashire	-1.3 ± 1.6	0
All	11.5 ± 6.3	0.7 ± 0.3

lines within that basin (Table 7). The highest values were recorded for the Vale of Eden and for Lancashire the fault was not significantly different from the control. When the possibility of the faults being sinks and the Vale of Eden data were removed from consideration then three faults showed fluxes significantly greater than zero.

4. Discussion

Methane concentrations were detected across fault and control routes, but time and resource constraints did not allow for monitoring of seasonal variation, potentially limiting the number of detects from faults. Moreover, due to practical constraints it was not possible to conduct the surveys at night time, when atmospheric conditions were more stable and may have allowed for a greater sensitivity of detection of fault sources. Methanotrophic oxidation of CH₄ are likely to reduce at night time, further increasing the likelihood that elevated concentrations of CH₄ could be detected - thus the number of detects from fault zones may be underrepresented. Furthermore, over 170 petroleum seepages have been identified across onshore Great Britain (Selley, 1992), with many associated with faults. Given that these would be point sources focused along particular faults rather than spread over a diffuse area, it is likely that the sampling regime has underrepresented the amount of CH₄ leakage occurring from fluid migration along fault zones. Due to time constraints it was necessary to conduct isotopic measurements on a subsequent day to the survey day, meaning meteorological conditions did not always allow comparable wind directions to previously identified areas of interest.

Monitoring fugitive CH₄ emissions using real-time mobile monitoring equipment raised interesting questions as to how best the dataset could be analysed. At the quantitative level this study identified sites of fugitive emissions based upon identifying a methane peak along the fault, a methane peak not within an urban area or near obvious sites of methane such as landfills; with the wind in the correct direction and an isotopic signal consistent with a thermogenic source. Two quantitative approaches were used, binary logistic regression and ANOVA. Binary logistic regression separated elevated concentrations from background concentrations, using the 90th percentile as a determinant for

what constituted an elevated concentration, based on previous work by Jackson et al. (2014), though their threshold was at 2.5 ppmv. This approach demonstrated the importance of landfill to fugitive emissions but suggested there was no significant difference between fault and control routes beyond that. Analysis of variance was more sensitive and given the experiment was set-up as a factorial design, ANOVA could identify significant differences between fault and control routes. Two approaches were used to determine methodological approaches for statistical analysis of mobile surveys and, ANOVA was a more appropriate measure of determining significance than binary logistic regression.

Results indicated that CH₄ migration from deep sources through preferential pathways caused by fault zones was significant, although there was no significant difference detected whether the basin was shale, non-shale hydrocarbon or non-hydrocarbon. Other studies have demonstrated the capacity for CH₄ migration in coal basins, including Thielemann et al. (2000) and Alsaab et al. (2009). Thielemann et al. (2000) reported thermogenic CH₄ in the range of –45 to –32‰ δ¹³-CH₄ in the eastern Ruhr Basin, while Alsaab et al. (2009) reported a range of –75 to –22‰ δ¹³-CH₄ in the Donets Basin. Here, a CH₄ signature was identified along the 90 Fathom fault (from one out of four significant isotope Keeling plots on the 90 Fathom fault route) with an isotopic value of –37‰ δ¹³-CH₄, displaying the isotopic enrichment associated with a thermogenic source. Thielemann et al. (2000) noted that CH₄ migration along natural faults was not widespread in the Ruhr Basin and was only focused in areas where coal gas accumulations were at the top of Carboniferous sediments. Baciu et al. (2008) also noted CH₄ seepage in Romania and suggested that seepage was only channelled at a few locations and was not widespread across the entire fault system. Thus, seepage along the 90 Fathom fault may not be widespread but focused in certain areas.

In Italy, a fault system was connected to a magma body, supporting a geothermal system with emissions of CO₂ of 3200 t/year as well as smaller emissions of other gases including CH₄ (Nuccio et al., 2014). Tang et al. (2010, 2013) noted enhanced CH₄ microseepage along faults in the Yakela condensed gas field, with increasing isotopic enrichment during flux measurements. Geothermal areas have been associated with thermogenic methane. Etiope et al. (2007) document 30 seeps (only 16 that were confirmed with isotopic analysis) in Italy all of which are associated with tectonic or neotectonic faults. Macroseeps (those with an identifiable vent) gave fluxes up to 2400 t CH₄/yr, whereas microseepage (assessed from soil gas measurements) gave an average CH₄ flux of 0.2 t CH₄/km²/yr over an area of 150,000 km². Etiope et al. (2007) note that natural seeps (both macro and micro) are one tenth the size of methane emissions from the entire Italian fossil fuel industry and its distribution network. Thielemann et al. (2000) reported thermogenic methane from Ruhr coalfields and Judd et al. (2002) associated the only other UK onshore gas seep as being from coal measures – they give a value of 40 kg CH₄/m²/yr for an area of 2400 m². Globally, Kvenvolden and Rogers (2005) have reported geological seepages of all types to be 45 Mt CH₄/yr, and Etiope and Klusman (2010) have estimated flux of thermogenic CH₄ to be between 40 and 60 Mt CH₄/yr. Geological sources of methane are now included in IPCC global assessments (Denman et al., 2007) with geological sources representing 9% of the global total emission.

The problem of upscaling results from this study is that the number of deep basin bounding faults in the UK is not known. Across Europe, geological seepage of CH₄ has been estimated at 3 Mt/yr, with 2.2 Mt/yr from macroseepage (mud volcanoes and other gas seeps) and 0.8 Mt/yr from microseepage (flux from soil, Etiope, 2009). With respect to this study we would classify the sources detected on faults as microseepage. Globally, onshore macroseepage has been suggested to be between 3 and 4 Mt/yr with diffuse soil microseepage between 10 and 25 Mt/yr (Etiope et al., 2011). Total global geologic CH₄ emission was estimated between 42 and 64 Mt/yr, representing between 19 and 27% of total global terrestrial CH₄ emissions of between ~280 Mt/yr,

with wetlands the largest source of modern microbial CH₄ (Etiope et al., 2011). The UK represents 5.6% of the European Union land area which would mean that pro rata the UK would be expected to be a source of 170 kt CH₄/yr from faults and given the figures measured in this study (if the Vale of Eden is included) then this would come from 15,178 km of fault. The most conservative estimate of CH₄ from basin bounding faults was 0.7 t CH₄/km/yr. Lifecycle emissions from shale gas had an expected range of 200–253 g CO₂eq/kWh, while this was 423–535 g CO₂eq/kWh(e) when compared to coal at 837–1130 g CO₂eq/kWh(e) for electricity generation (e) rather than chemical energy (MacKay and Stone, 2013). The fault emissions factor would be 16.8 t CO₂eq/km/yr. By comparison to agriculture, a breeding ewe has an emission factor of 209 kg CO₂eq/head/year, with 21 sheep per hectare of lowland agriculture in the UK.

Faults in the UK have been shown to be sources of CH₄, though this is not the case for all basin bounding faults. However, the question as to whether hydrofracturing as part of shale gas development will cause transmission of gases through major faults to increase has not been addressed here. Numerous factors would affect the propensity for CH₄ in shale basins to migrate to the surface along fault zones. There is no evidence of overpressure in onshore UK basins, (Harvey and Gray, 2013), in part this may be due to uplift reducing any overpressure over time. Productivity in an overpressured system would likely deliver more gas than a normal pressured (equivalent to hydrostatic pressure) system. Furthermore, the likelihood of CH₄ migration along permeable pathways would be reduced if there was limited pressure driving fluid flow. Secondly, the behaviour of shales will vary depending upon its mechanical properties and mineralogy. For instance, the Whitby Mudstone Formation has silicate content of 13–18% with high clay content and low quartz and carbonate content and the brittleness index suggests it is in the ductile to less ductile regime (Houben et al., 2016). The Whitby Mudstone Formation may consequently be less liable to fracture than other shales, while porosity is also low for gas transportation (Houben et al., 2016). The elastic properties of Barnett, Haynesville, Eagle Ford and Fort St. John shales have been shown to vary between and within reservoirs, with anisotropy related to clay and organic content as some shales show strong fabric anisotropy, while others do not (Sone and Zoback, 2013). Thus, different reservoirs will have different capacities for both production and fluid migration along permeable pathways, while this would also be expected to change as reservoirs become depleted during production and effective stress alters shale permeability, though slippage effects at low pore pressures could offset some decreases in permeability (Heller et al., 2014).

The largest emissions of CH₄ emanated from a landfill site and most isotopic sources were identified as biogenic, indicating microbial sources of CH₄ were important. Lan et al. (2015) reported a range of 3.25–14.76 ppmv CH₄ from landfills, similar to the 13.73 ppmv CH₄ found on the 90 Fathom route. The isotopic value of –61‰ δ¹³-CH₄ was also similar to that reported for landfill gas of –61.5 and –61.9‰ δ¹³-CH₄ in Los Angeles (Townsend-Small et al., 2012). Four thermogenic signatures were not associated with a fault (–37 to –41‰ δ¹³-CH₄) and may have been from local gas pipeline leaks. Phillips et al. (2013) reported natural gas values of –36.8‰ ± 0.7‰ δ¹³-CH₄ for pipeline leaks across Boston while Jackson et al. (2014) reported isotopic values of –38.2‰ ± 3.9‰ δ¹³-CH₄ for pipeline leaks across Washington, DC. The maximum concentration recorded here was 12.30 ppmv CH₄ on the Widmerpool control; on the Vale of Eden control it was 10.05 ppmv CH₄. Phillips et al. (2013) reported a maximum of 28.6 ppmv CH₄ in Boston while Gallagher et al. (2015) reported a maximum of 88.6 ppmv CH₄ across five cities, with the highest from Washington, DC (Jackson et al., 2014). Thus, whether from biological sources such as farms and landfill or natural gas pipeline sources, high concentrations of fugitive CH₄ were identified in this study that were not associated with fault-derived migration that also represented a significant source to the atmosphere.

5. Conclusions

Basin bounding faults in the UK could be significant conduits for CH₄. Some basins did not have a significant flux of CH₄, but in general, and as the most conservative estimate, basin bounding faults represent a flux of methane to the atmosphere of 0.7 ± 0.5 t CH₄/km/yr. Emissions from faults were not especially associated with faults bounding hydrocarbon basins, including potential shale gas basins. With this baseline data, future studies can assess the impact hydraulic fracturing processes have on methane emissions along fault zones.

Acknowledgements

This research was carried out as part of the ReFINE research consortium led by Newcastle and Durham Universities. ReFINE has been funded by Ineos, Shell, Chevron, Total, GDF Suez, Centrica and NERC. We thank the ReFINE Independent Science Board for prioritising the research projects undertaken by ReFINE.

Appendix A. Supplementary data

Supplementary data to this article can be found online at <http://dx.doi.org/10.1016/j.scitotenv.2016.09.052>.

References

- Alsaab, D., Elie, M., Izart, A., Sachsenhofer, R.F., Privalov, V.A., Suarez-Ruiz, I., Martinez, L., Panova, E.A., 2009. Distribution of thermogenic methane in Carboniferous coal seams of the Donets Basin (Ukraine): "applications to exploitation of methane and forecast of mining hazards". *Int. J. Coal Geol.* 78 (1), 27–37.
- Anderson, T.W., Darling, D.A., 1952. Asymptotic theory of certain goodness of fit criteria based on stochastic processes. *Ann. Math. Stat.* 23 (2), 193–212.
- Andrews, I.J., 2013. The Carboniferous Bowland Shale Gas Study: Geology and Resource Estimation. British Geological Survey for Department of Energy and Climate Change, London, UK.
- Baciu, C., Etiopie, G., Cuna, S., Spulber, L., 2008. Methane seepage in an urban development area (Bacau, Romania): origin, extent, and hazard. *Geofluids* 8 (4), 311–320.
- Beach, A., Brown, J.L., Welbon, A.L., McCallum, J.E., Brockbank, P., Knott, S., 1997. Characteristics of fault zones in sandstones from NW England: application to fault transmissibility. *Petroleum Geology of the Irish Sea and Adjacent Areas*. 124, pp. 315–324.
- Birdsell, D.T., Rajaram, H., Dempsey, D., Viswanathan, H.S., 2015. Hydraulic fracturing fluid migration in the subsurface: a review and expanded modeling results. *Water Resour. Res.* 51 (9), 7159–7188.
- Boardman, E., Rippon, J., 1997. Coalbed methane migration in and around fault zones. *Geol. Soc. Lond., Spec. Publ.* 125 (1), 391–408.
- Boothroyd, I.M., Almond, S., Qassim, S.M., Worrall, F., Davies, R.J., 2016. Fugitive emissions of methane from abandoned, decommissioned oil and gas wells. *Sci. Total Environ.* 547, 461–469.
- Brantley, H.L., Thoma, E.D., Squier, W.C., Guven, B.B., Lyon, D., 2014. Assessment of methane emissions from oil and gas production pads using mobile measurements. *Environ. Sci. Technol.* 48 (24), 14508–14515.
- British Geological Survey, 1969. Barnard Castle. England & Wales Sheet 32. Solid. 1:50 000. British Geological Survey, Keyworth, Nottingham.
- British Geological Survey, 1974. Penrith. England & Wales Sheet 24. Solid. 1:50 000. British Geological Survey, Keyworth, Nottingham.
- British Geological Survey, 1975. Hexham. England & Wales Sheet 19. Solid. 1:50 000. British Geological Survey, Keyworth, Nottingham.
- British Geological Survey, 1977. Wigan. England & Wales Sheet 84. Solid. 1:50 000. British Geological Survey, Keyworth, Nottingham.
- British Geological Survey, 1989. Newcastle Upon Tyne. England & Wales Sheet 20. Solid. 1:50 000. British Geological Survey, Keyworth, Nottingham.
- British Geological Survey, 2008. Durham. England & Wales Sheet 27. Bedrock. 1:50 000. British Geological Survey, Keyworth, Nottingham.
- British Geological Survey, 2012. Preston. England & Wales Sheet 75. Bedrock and Superficial Deposits. 1:50 000. British Geological Survey, Keyworth, Nottingham.
- Burnham, A., Han, J., Clark, C.E., Wang, M., Dunn, J.B., Palou-Rivera, I., 2012. Life-cycle greenhouse gas emissions of shale gas, natural gas, coal, and petroleum. *Environ. Sci. Technol.* 46 (2), 619–627.
- Burnside, N.M., Shipton, Z.K., Dockrill, B., Ellam, R.M., 2013. Man-made versus natural CO₂ leakage: a 400 k.y. history of an analogue for engineered geological storage of CO₂. *Geology* 41 (4), 471–474.
- Church, K.D., Gawthorpe, R.L., 1994. High-resolution sequence stratigraphy of the late Namurian in the widmerpool gulf (east midlands, UK). *Mar. Pet. Geol.* 11 (5), 528–544.
- Creedy, D.P., 1988. Geological controls on the formation and distribution of Gas in British-Coal Measure Strata. *Int. J. Coal Geol.* 10 (1), 1–31.
- Darrah, T.H., Vengosh, A., Jackson, R.B., Warner, N.R., Poreda, R.J., 2014. Noble gases identify the mechanisms of fugitive gas contamination in drinking-water wells overlying the Marcellus and Barnett Shales. *Proc. Natl. Acad. Sci. U. S. A.* 111 (39), 14076–14081.
- Davies, R.J., Mathias, S.A., Moss, J., Hustoft, S., Newport, L., 2012. Hydraulic fractures: how far can they go? *Mar. Pet. Geol.* 37 (1), 1–6.
- Davies, R.J., Foulger, G.R., Mathias, S., Moss, J., Hustoft, S., Newport, L., 2013. Reply: Davies et al. (2012a), Hydraulic fractures: how far can they go? *Mar. Pet. Geol.* 43, 519–521.
- Davies, R.J., Almond, S., Ward, R.S., Jackson, R.B., Adams, C., Worrall, F., Herringshaw, L., Gluyas, J.G., Whitehead, M.A., 2014. Oil and gas wells and their integrity: implications for shale and unconventional resource exploitation. *Mar. Pet. Geol.* 56, 239–254.
- De Paola, N., Holdsworth, R.E., McCaffrey, K.J.W., 2005. The influence of lithology and pre-existing structures on reservoir-scale faulting patterns in transtensional rift zones. *J. Geol. Soc.* 162, 471–480.
- Denman, K.L., Brasseur, G., Chidthaisong, A., Ciais, P., Cox, P.M., Dickinson, R.E., Hauglustaine, D., Heinze, C., Holland, E., Jacob, D., Lohmann, U., Ramachandran, S., da Silva Dias, P.L., Wofsy, S.C., Zhang, X., 2007. Couplings between changes in the climate system and biogeochemistry. In *Climate Change 2007: The Physical Science Basis. Contribution of Working Group I to the Fourth Assessment Report of the Intergovernmental Panel on Climate Change* (eds S. Solomon, D. Qin, M. Manning, Z. Chen, M. Marquis, K.B. Averyt, M. Tignor H.L. Miller), pp. 499–587. Cambridge University Press, Cambridge, United Kingdom.
- Dockrill, B., Shipton, Z.K., 2010. Structural controls on leakage from a natural CO₂ geologic storage site: Central Utah, USA. *J. Struct. Geol.* 32 (11), 1768–1782.
- Duncan, W.I., Green, P.F., Duddy, I.R., 1998. Source rock burial history and seal effectiveness: key facets to understanding hydrocarbon exploration potential in the East and Central Irish Sea Basins. *Aapg Bulletin-American Association of Petroleum Geologists* 82 (7), 1401–1415.
- Etiopie, G., 1999. Subsoil CO₂ and CH₄ and their advective transfer from faulted grassland to the atmosphere. *Journal of Geophysical Research: Atmospheres* (1984–2012) 104 (D14), 16889–16894.
- Etiopie, G., 2009. Natural emissions of methane from geological seepage in Europe. *Atmos. Environ.* 43 (7), 1430–1443.
- Etiopie, G., Klusman, R.W., 2002. Geologic emissions of methane to the atmosphere. *Chemosphere* 49 (8), 777–789.
- Etiopie, G., Klusman, R.W., 2010. Microseepage in drylands: flux and implications in the global atmospheric source/sink budget of methane. *Global Planet. Change* 72 (4), 265–274.
- Etiopie, G., Martinelli, G., Caracausi, A., Italiano, F., 2007. Methane seeps and mud volcanoes in Italy: gas origin, fractionation and emission to the atmosphere. *Geophys. Res. Lett.* 34 (14).
- Etiopie, G., Oehler, D.Z., Allen, C.C., 2011. Methane emissions from Earth's degassing: implications for Mars. *Planet. Space Sci.* 59 (2–3), 182–195.
- Fairley, J.P., Hinds, J.J., 2004. Rapid transport pathways for geothermal fluids in an active Great Basin fault zone. *Geology* 32 (9), 825–828.
- Fielding, C.R., 1984. A coal depositional model for the Durham coal measures of NE England. *Journal of the Geological Society* 141 (SEP), 919–931.
- Fraser, A.J., Nash, D.F., Steele, R.P., Ebdon, C.C., 1990. A regional assessment of the intra-carboniferous play of northern England. *Classic Petroleum Provinces* 50, 417–440.
- Gallagher, M.E., Down, A., Ackley, R.C., Zhao, K.G., Phillips, N., Jackson, R.B., 2015. Natural gas pipeline replacement programs reduce methane leaks and improve consumer safety. *Environ. Sci. Technol. Lett.* 2 (10), 286–291.
- Grasby, S.E., Ferguson, G., Brady, A., Sharp, C., Dunfield, P., McMechan, M., 2016. Deep groundwater circulation and associated methane leakage in the northern Canadian Rocky Mountains. *Appl. Geochem.* 68, 10–18.
- Harvey, T., Gray, J., 2013. The Unconventional Hydrocarbon Resources of Britain's Onshore Basins–Shale Gas. Rep. Dept. Energy Climate Change.
- Heller, R., Vermeylen, J., Zoback, M., 2014. Experimental investigation of matrix permeability of gas shales. *AAPG Bull.* 98 (5), 975–995.
- Hensen, A., Scharff, H., 2001. Methane emission estimates from landfills obtained with dynamic plume measurements. *Water, Air and Soil Pollution, Focus* 1 (5), 455–464.
- Hosmer, D.W., Lemeshow, S., 2000. *Applied Logistic Regression*. 2nd ed. Wiley, New York; Chichester.
- Houben, M.E., Barnhoorn, A., Lie-A-Fat, J., Ravestein, T., Peach, C.J., Drury, M.R., 2016. Microstructural characteristics of the Whitby Mudstone Formation (UK). *Mar. Pet. Geol.* 70, 185–200.
- Howarth, R.W., Santoro, R., Ingrassia, A., 2011. Methane and the greenhouse-gas footprint of natural gas from shale formations. *Clim. Change* 106 (4), 679–690.
- Ingrassia, A.R., Wells, M.T., Santoro, R.L., Shonkoff, S.B.C., 2014. Assessment and risk analysis of casing and cement impairment in oil and gas wells in Pennsylvania, 2000–2012. *Proc. Natl. Acad. Sci. U. S. A.* 111 (30), 10955–10960.
- Jackson, D.I., Mulholland, P., 1993. Tectonic and stratigraphic aspects of the east Irish sea basin and adjacent areas - contrasts in their post-carboniferous structural styles. *Petroleum Geology of Northwest Europe: Proceedings of the 4th Conference*, pp. 791–808.
- Jackson, R.B., Down, A., Phillips, N.G., Ackley, R.C., Cook, C.W., Plata, D.L., Zhao, K.G., 2014. Natural gas pipeline leaks across Washington, DC. *Environ. Sci. Technol.* 48 (3), 2051–2058.
- Jackson, R.B., Lowry, E.R., Pickle, A., Kang, M., DiGiulio, D., Zhao, K.G., 2015. The depths of hydraulic fracturing and accompanying water use across the United States. *Environ. Sci. Technol.* 49 (15), 8969–8976.
- Judd, A.G., Sim, R., Kingston, P., McNally, J., 2002. Gas seepage on an intertidal site: Torry Bay, Firth of Forth, Scotland. *Cont. Shelf Res.* 22, 2317–2331.
- Kang, M., Kanno, C.M., Reid, M.C., Zhang, X., Mauzerall, D.L., Celia, M.A., Chen, Y., Onstott, T.C., 2014. Direct measurements of methane emissions from abandoned oil and gas wells in Pennsylvania. *Proc. Natl. Acad. Sci.* 111 (51), 18173–18177.

- Kissinger, A., Helmig, R., Ebigbo, A., Class, H., Lange, T., Sauter, M., Heitfeld, M., Klunker, J., Jahnke, W., 2013. Hydraulic fracturing in unconventional gas reservoirs: risks in the geological system, part 2. *Environ. Earth Sci.* 70 (8), 3855–3873.
- Knott, S.D., 1994. Fault zone thickness versus displacement in the permo-Triassic sandstones of NW England. *J. Geol. Soc.* 151, 17–25.
- Kortas, L., Younger, P.L., 2013. Fracture patterns in the Permian Magnesian Limestone Aquifer, Co. Durham, UK. *Proc. Yorks. Geol. Soc.* 59 (3), 161–171.
- Kotarba, M.J., Nagao, K., Karnkowski, P.H., 2014. Origin of gaseous hydrocarbons, noble gases, carbon dioxide and nitrogen in Carboniferous and Permian strata of the distal part of the Polish Basin: geological and isotopic approach. *Chem. Geol.* 383, 164–179.
- Kvenvolden, K.A., Rogers, B.W., 2005. Gaia's breath – global methane exhalations. *Mar. Pet. Geol.* 22 (4), 579–590.
- Lan, X., Talbot, R., Laine, P., Torres, A., 2015. Characterizing fugitive methane emissions in the Barnett shale area using a mobile laboratory. *Environ. Sci. Technol.* 49 (13), 8139–8146.
- Lange, T., Sauter, M., Heitfeld, M., Schetelig, K., Brosig, K., Jahnke, W., Kissinger, A., Helmig, R., Ebigbo, A., Class, H., 2013. Hydraulic fracturing in unconventional gas reservoirs: risks in the geological system part 1. *Environ. Earth Sci.* 70 (8), 3839–3853.
- Lavoie, D., Pinet, N., Bordeleau, G., Ardakani, O.H., Ladeveze, P., Duchesne, M.J., Rivard, C., Mort, A., Brake, V., Sanei, H., Malet, X., 2016. The Upper Ordovician black shales of southern Quebec (Canada) and their significance for naturally occurring hydrocarbons in shallow groundwater. *Int. J. Coal Geol.* 158, 44–64.
- Llewellyn, G.T., Dorman, F., Westland, J.L., Yoxheimer, D., Grieve, P., Sowers, T., Humston-Fulmer, E., Brantley, S.L., 2015. Evaluating a groundwater supply contamination incident attributed to Marcellus Shale gas development. *Proc. Natl. Acad. Sci.* 112 (20), 6325–6330.
- Mackay, D.J.C., Stone, T.J., 2013. Potential Greenhouse Gas Emissions Associated with Shale Gas Extraction and Use. Dept. of Energy & Climate Change, London, UK.
- Maher, D.T., Santos, I.R., Tait, D.R., 2014. Mapping methane and carbon dioxide concentrations and delta C-13 values in the atmosphere of two Australian coal seam gas fields. *Water Air Soil Pollut.* 225 (12).
- Molofsky, L.J., Connor, J.A., Farhat, S.K., Wylie Jr., A.S., Wagner, T., 2011. Methane in Pennsylvania water wells unrelated to Marcellus shale fracturing. *Oil Gas J.* 109 (19), 54–67.
- Moritz, A., Helie, J.F., Pinti, D.L., Larocque, M., Barnetche, D., Retailleau, S., Lefebvre, R., Gelin, Y., 2015. Methane baseline concentrations and sources in shallow aquifers from the shale gas-prone region of the St. Lawrence Lowlands (Quebec, Canada). *Environ. Sci. Technol.* 49 (7), 4765–4771.
- Neymeyer, A., Williams, R.T., Younger, P.L., 2007. Migration of polluted mine water in a public supply aquifer. *Q. J. Eng. Geol. Hydrogeol.* 40, 75–84.
- Nuccio, P.M., Caracausi, A., Costa, M., 2014. Mantle-derived fluids discharged at the Bradanic foredeep/Apulian foreland boundary: the Maschito geothermal gas emissions (southern Italy). *Mar. Pet. Geol.* 55, 309–314.
- O'Donoghue, P.R., Heath, G.A., Dolan, S.L., Vorum, M., 2014. Life cycle greenhouse gas emissions of electricity generated from conventionally produced natural gas systematic review and harmonization. *J. Ind. Ecol.* 18 (1), 125–144.
- Olejnik, S., Algina, J., 2003. Generalized eta and omega squared statistics: measures of effect size for some common research designs. *Psychol. Methods* 8 (4), 434–447.
- Osborne, M.J., Swarbrick, R.E., 1997. Mechanisms for generating overpressure in sedimentary basins: a reevaluation. *AAPG Bull.* 81 (6), 1023–1041.
- O'Sullivan, F., Paltsev, S., 2012. Shale gas production: potential versus actual greenhouse gas emissions. *Environ. Res. Lett.* 7 (4).
- Pataki, D.E., Ehleringer, J.R., Flanagan, L.B., Yakir, D., Bowling, D.R., Still, C.J., Buchmann, N., Kaplan, J.O., Berry, J.A., 2003. The application and interpretation of keeling plots in terrestrial carbon cycle research. *Global Biogeochem. Cycles* 17 (1), 1022. <http://dx.doi.org/10.1029/2001gb001850>.
- Phillips, N.G., Ackley, R., Crosson, E.R., Down, A., Hutyra, L.R., Brondfield, M., Karr, J.D., Zhao, K.G., Jackson, R.B., 2013. Mapping urban pipeline leaks: methane leaks across Boston. *Environ. Pollut.* 173, 1–4.
- Reagan, M.T., Moridis, G.J., Keen, N.D., Johnson, J.N., 2015. Numerical simulation of the environmental impact of hydraulic fracturing of tight/shale gas reservoirs on near-surface groundwater: background, base cases, shallow reservoirs, short term gas, and water transport. *Water Resour. Res.* 51 (4), 2543–2573.
- Selley, R.C., 1992. Petroleum seepages and impregnations in Great Britain. *Mar. Pet. Geol.* 9 (3), 226–244.
- Sone, H., Zoback, M.D., 2013. Mechanical properties of shale-gas reservoir rocks – part 1: static and dynamic elastic properties and anisotropy. *Geophysics* 78 (5), D378–D389.
- Stewart, S.A., Davies, R.J., 2006. Structure and emplacement of mud volcano systems in the South Caspian Basin. *AAPG Bull.* 90 (5), 771–786.
- Tang, J.H., Yin, H.Y., Wang, G.J., Chen, Y.Y., 2010. Methane microseepage from different sectors of the Yakela condensed gas field in Tarim Basin, Xinjiang, China. *Appl. Geochem.* 25 (8), 1257–1264.
- Tang, J., Wang, G., Yin, H., Li, H., 2013. Methane in soil gas and its transfer to the atmosphere in the Yakela condensed gas field in the Tarim Basin, Northwest China. *Pet. Sci.* 10 (2), 183–189.
- Thielemann, T., Lucke, A., Schleser, G.H., Littke, R., 2000. Methane exchange between coal-bearing basins and the atmosphere: the Ruhr Basin and the Lower Rhine Embayment, Germany. *Org. Geochem.* 31 (12), 1387–1408.
- Townsend-Small, A., Tyler, S.C., Pataki, D.E., Xu, X.M., Christensen, L.E., 2012. Isotopic measurements of atmospheric methane in Los Angeles, California, USA: influence of "fugitive" fossil fuel emissions. *J. Geophys. Res.-Atmos.* 117.
- Townsend-Small, A., Ferrara, T.W., Lyon, D.R., Fries, A.E., Lamb, B.K., 2016. Emissions of coalbed and natural gas methane from abandoned oil and gas wells in the United States. *Geophys. Res. Lett.* 43 (5), 2283–2290.
- Underhill, J.R., Gayer, R.A., Woodcock, N.H., Donnelly, R., Jolley, E.J., Stimpson, I.G., 1988. The dent fault system, northern England – reinterpreted as a major oblique-slip-fault zone. *J. Geol. Soc.* 145, 303–316.
- Voltattomi, N., Cinti, D., Pizzino, L., Sciarra, A., 2014. Statistical approach for the geochemical signature of two active normal faults in the western Corinth Gulf Rift (Greece). *Appl. Geochem.* 51, 86–100.
- Warner, N.R., Jackson, R.B., Darrach, T.H., Osborn, S.G., Down, A., Zhao, K.G., White, A., Vengosh, A., 2012. Geochemical evidence for possible natural migration of Marcellus Formation brine to shallow aquifers in Pennsylvania. *Proc. Natl. Acad. Sci. U. S. A.* 109 (30), 11961–11966.
- Whitcar, M.J., 1999. Carbon and hydrogen isotope systematics of bacterial formation and oxidation of methane. *Chem. Geol.* 161 (1), 291–314.